www.contempclindent.org
DOI: 10.4103/0976-237X.72781

X-Ray diffraction and scanning electron microscopy-energy dispersive spectroscopic analysis of ceramometal interface at different firing temperatures

Monika Saini[1], Suresh Chandra[2], Yashpal Singh[3], Bikramjit Basu[4], Arvind Tripathi[5]

Abstract

Objective: *Porcelain chipping* from porcelain fused to metal restoration has been Achilles heel till date. There has been advent of newer ceramics in past but but none of them has been a panacea for Porcelain fracture. An optimal firing is thus essential for the clinical success of the porcelain-fused to metal restoration. The aim of the present study was to evaluate ceramo-metal interface at different firing temperature using XRD and SEM-EDS analysis. Clinical implication of the study was to predict the optimal firing temperature at which porcelain should be fused with metal in order to possibly prevent the occasional failure of the porcelain fused to metal restorations. **Materials and Methods:** To meet the above-mentioned goal, porcelain was fused to metal at different firing temperatures (930–990°C) in vacuum. The microstructural observations of interface between porcelain and metal were evaluated using X-ray diffraction and scanning electron microscopy with energy dispersive spectroscopy. **Results:** Based on the experimental investigation of the interaction zone of porcelain fused to metal samples, it was observed that as the *firing temperature* was increased, the pores became less in number as well as the size of the pores decreased at the porcelain/metal interface upto 975°C but increased in size at 990°C. The least number of pores with least diameter were found in samples fired at 975°C. Several oxides like Cr_2O_3, NiO, and Al_2O_3 and intermetallic compounds ($CrSi_2$, $AlNi_3$) were also formed in the interaction zone. **Conclusions**: It is suggested that the presence of pores may trigger the crack propagation along the interface, causing the failure of the porcelain fused to metal restoration during masticatory action.

Keywords: Firing temperature, porcelain chipping, pores

Introduction

Occasional chipping of porcelain from metal surface in PFM restorations has been the continued problem till date. The failure of porcelain–metal bond leads to restoration failure. This failure can occur cohesively within porcelain, in metal or at porcelain–metal interface. Several studies have been conducted to determine the strength of porcelain–metal bonds[1-10] porcelain–metal interface,[11-15] fracture resistance of Porcelain Fused to Metal restorations,[16,17] porcelain-metal thermal compatibility,[18] effect of heat treatment and firing cycle,[19-21] adhesion of porcelain to other metal[22,23]. Present study deals with failure of porcelain metal interface. Porcelain fused to metal restoration failure can occur due to multiple reasons. This paper will focus on the effect of various firing temperatures on porcelain–metal interface.

Poorly controlled firing temperature is supposed to be potential cause to PFM restoration failure. An optimal firing temperature for porcelain is supposed to be one of the major factors for the restorations to be clinically successful. The aim of this study was to characterize the microstructure of oxide layer formed on metal surface before firing and after firing the PFM samples at different firing temperatures. The interaction zone formed along the interface was studied and evaluated.

The objective of the study was to predict the optimal firing temperature at which porcelain should be fused with metal in PFM restorations.

Material and Method

Casting of base metal alloy

Casting of base metal alloy was done [Chart 1]. Sample A was casted but not oxidised.Sample B was casted,oxidised but Porcelain was not applied.Sample C to G were casted, oxidised and Porcelain was applied.All the samples were evaluated microstructurally [Chart 2]. X-ray diffraction was done for Sample A,B and control sample. XRD and SEM-EDS analysis was done for samples C to G.

Results and Discussion

Porcelain fused to metal sample preparation (Samples C to G)

Figure 1 showed the relative X-ray diffraction (XRD) patterns for commercial base metal alloy (Niadur), Sample A and Sample B. Commercial base metal alloy showed the presence of delta phase chromium, nickel [δ(Cr, Ni)] in it.

[1,3]*Department of Prosthodontics, Subharti Dental College, Meerut,*
[2]*Department of Prosthodontics, DJ Dental College, Modinagar,*
[4]*Department of Metallurgy, Indian Institute of Technology, Kanpur,*
[5]*Department of Prosthodontics, Saraswati Dental College, Lucknow, India*

Correspondence: Dr. Yashpal Singh,
H. no. 35, Sector 11, UNI Apartments, Vasundhara, Ghaziabad, U.P.- 201 012, India. E-mail: dryashpal.singh@gmail.com

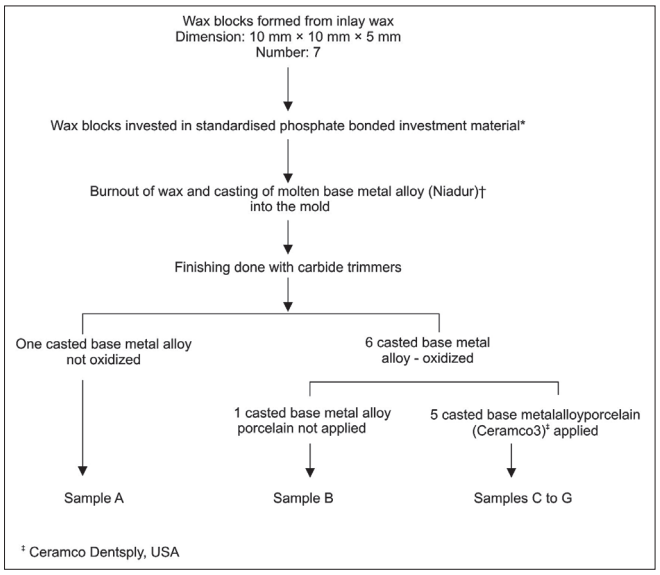

Chart 1: Casting of Base Metal Alloy.
*Begosol, Bego, Germany †NIOM – Made in Germany, DFS

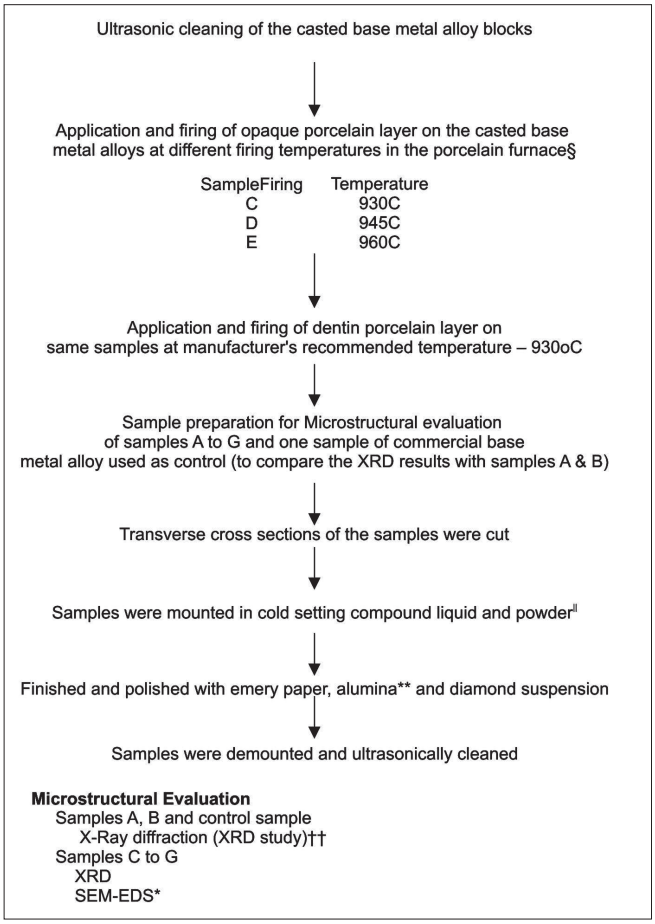

Chart 2: Microstructural evaluation of sample.
§Lectra, UGIN, France, ||KRISH (Cold setting compound liquid and powder) for metallurgical specimen mounting, Chennai, ¨Emery Paper No. 1/0,2/0, 3/0 <SIA> 1600 SAINOR B Swiss made; Emery Paper No. 4/0, John Oakey and Sons Limited, Made in England, ††ISO-DEBYEFLEX-2002, Germany *JEOL JSM-840

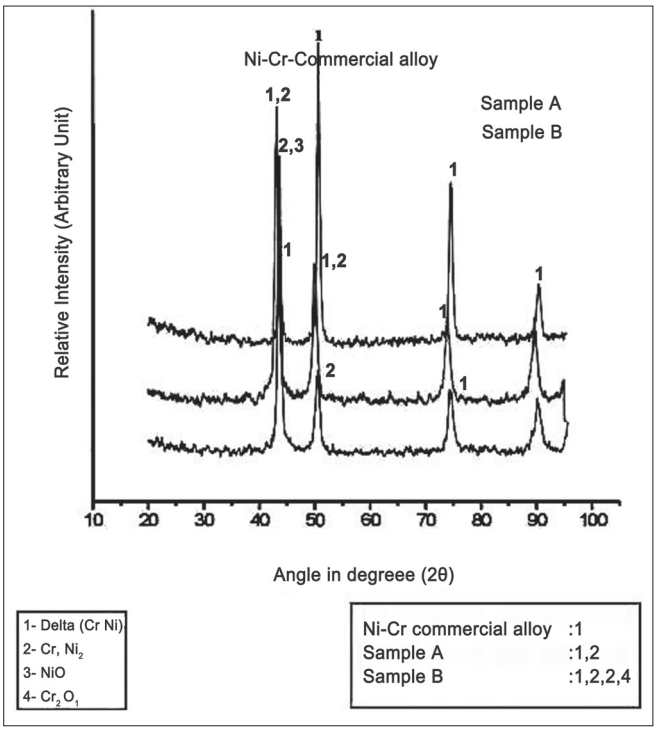

Figure 1: Relative X-ray diffraction analysis for commercial base metal alloy sample, Sample A and sample B

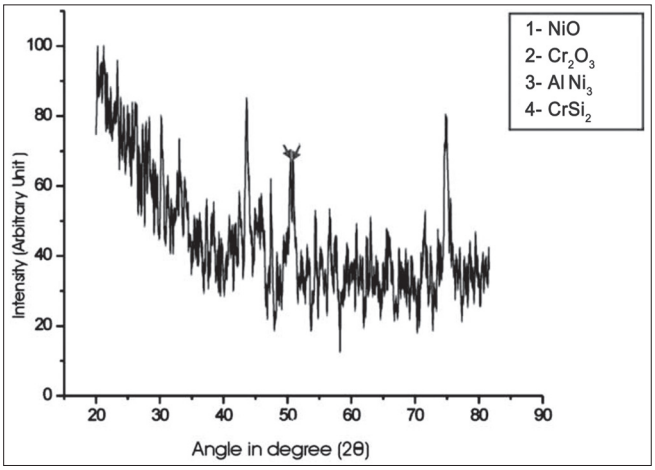

Figure 2: Diffraction pattern for sample C (opaque layer fired at 930°C)

Sample A showed the presence of intermetallic compound Cr_3Ni_2 besides δ (Cr, Ni) phase whereas Sample B showed the presence of Cr_3Ni_2, nickel oxide (NiO), chromium oxide (Cr_2O_3) and delta phase. Since this sample was oxidized, the formation of these metallic oxides was quite reasonable.

The XRD pattern [Figures 2-6] and EDS patterns were recorded for samples C to G. [Table 1] shows the various oxides and inter metallic compounds formed in different samples and [Table 2] shows distribution of major elements

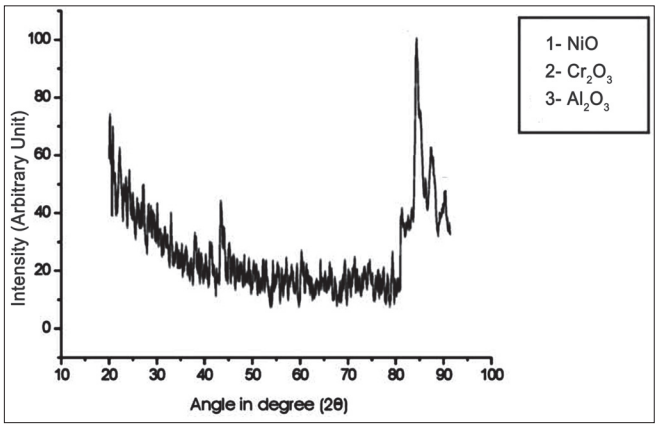

Figure 3: Diffraction pattern for sample D (opaque layer fired at 945°C)

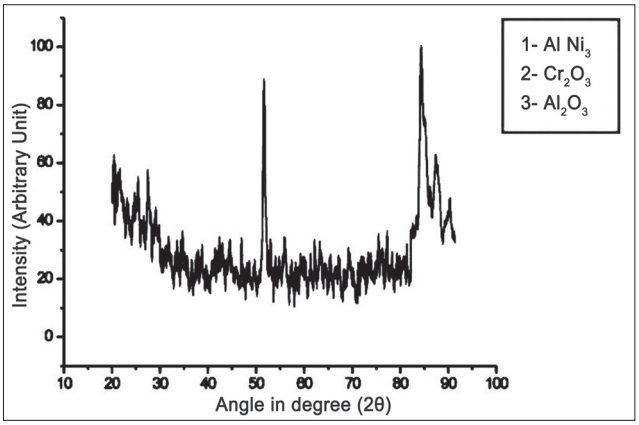

Figure 4: Diffraction pattern for sample E (opaque layer fired at 960°C)

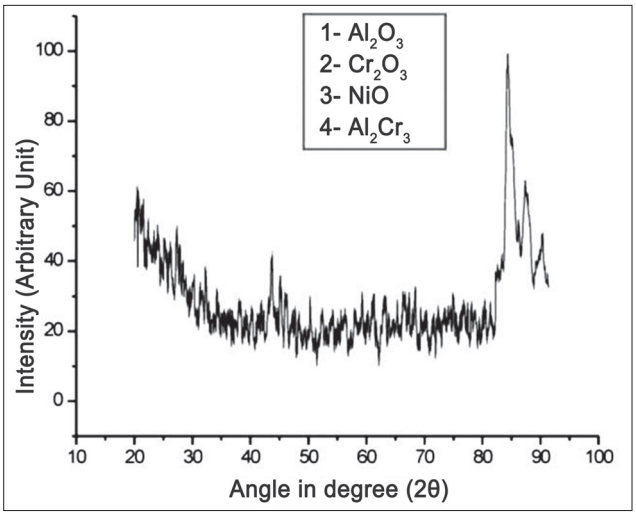

Figure 5: Diffraction pattern for sample F (opaque layer fired at 975°C)

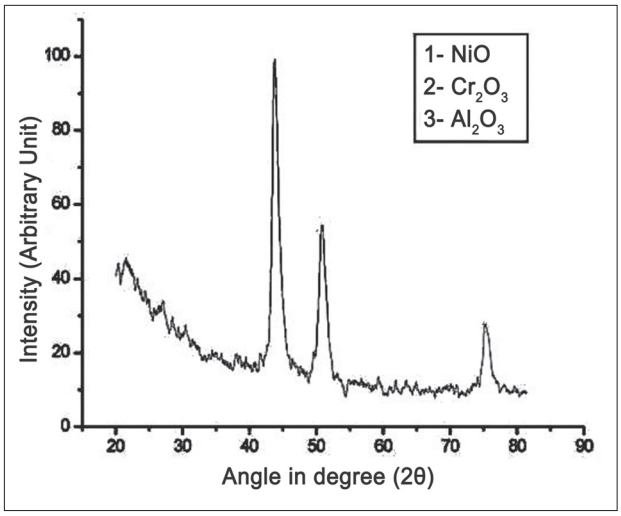

Figure 6: Diffraction pattern for sample G (opaque layer fired at 990°C)

X-RAY DIFFRACTION (XRD) OBSERVATIONS

Table 1: Oxides and intermetallic compounds formed in different samples

Sample	Oxides	Intermetallic compounds
Commercial base-metal alloy	–	Delta (Cr, Ni)
Sample A	–	Cr_3Ni_2, Delta (Cr, Ni)
Sample B	NiO, Cr_2O_3	Cr_3Ni_2, Delta (Cr, Ni)
Sample C	NiO, Cr_2O_3	$CrSi_2$, $AlNi_3$
Sample D	Al_2O_3, Cr_2O_3, NiO	–
Sample E	Al_2O_3, Cr_2O_3	$AlNi_3$
Sample F	Al_2O_3, Cr_2O_3, NiO	Al_2Cr_3
Sample G	Cr_2O_3, NiO, Al_2O_3	–

observed in SEM-EDS analysis. The EDS analysis was recorded in the region around the interface of metal and porcelain, at an interval of 20 μm on either side of interface. This region formed the integral part of the interaction zone.

Table 2: Distribution of major elements observed in SEM-EDS analysis

Sample	Interface region	Metal region	Porcelain region
C	Ni, Cr, O	Ni, Cr, O	Si, Al, K, O
D	Al, Ni, Cr, O	Ni, Cr, O	Si, Al, K, O
E	Ni, Cr, Al	Ni, Cr	Si, Al, K
F	Si, Al, O, Cr	Ni, Cr, O	Si, Al, O
G	Ni, Cr, O	Ni, Cr, O	Si, Al, K, O

The EDS analysis was done for elemental recordings at the locations described above. The results were qualitatively correlated with XRD observations, which led to the evaluation of interaction zone.

Samples C–G showed the presence of oxides of Ni, Cr, and Al. Various intermetallic compounds like $CrNi_2$, $CrSi_2$, $AlNi_3$, and Al_2Cl_3 were also formed.

Sample E observations were well supported by the findings of Anusavice (1977) who showed Ni–Cr interactions with ceramic complexes. The presence of Al_2Cr_3 in Sample F further supported the studies of KJ Anusavice, RD Ringle, and CW Fairhurst,[5] who showed the presence of predominant Al-Cr interactions. The Cr ions were supplied by Cr_2O_4 oxide layer of metal surface and Al was provided by porcelain surface.

The XRD pattern and EDS analysis of various samples from A to G reconfirmed the fact that the oxidation of casted commercial base metal alloy led to the formation of oxides of major elements present in it (Ni, Cr) and during firing, the major elements from porcelain (K, Si, Al) interacted with metal oxide to form various oxides and intermetallic compounds. This resulted in the formation of interaction zone between metal and porcelain.

SEM image [Figure 7] of porcelain fused to metal sample C (opaque porcelain layer fired at 930°C) showed large number of pores ranging from 25–30. The size of average diameter of observed pores was found to be 43 μm. These large-sized pores were triangular to irregular in shape [Figure 8]. This observation can be explained by the studies of Anusavice.[24] They observed that during firing, the voids between porcelain particles were occupied by the furnace atmosphere. The vacuum, created during firing, pushes the air out of the porcelain particles. During firing, porcelain particles bond at their point of contact as the sintering of porcelain particles occur. The sintered porcelain particles try to flow and fill up the pore spaces. It might be presumed that large number of pores in this sample were due to incomplete sintering of porcelain particles and inability of particles to flow and fill up the air spaces completely. This can be also predicted from the fact that the commercial porcelain, used in the present study, is usually densified/sintered in the temperature range of 850–1100°C. Therefore, it can be said that due to lower temperature of 930°C, the sintering of porcelain particles was not complete, which resulted in large-sized pore formation.

As the firing temperature was increased to 975°C (sample F), both the number of pore and average diameter of pores [Figure 9] and [Figure 10] decreased due to better fusion of porcelain particles. Also, the flow of particles was increased causing increased filling of air space among the particles. In sample G, the number of pore and average diameter of pores did not decrease because fusion ability of porcelain particle did not increase at this temperature and tend to remain constant. On the contrary, pore size was increased. It was

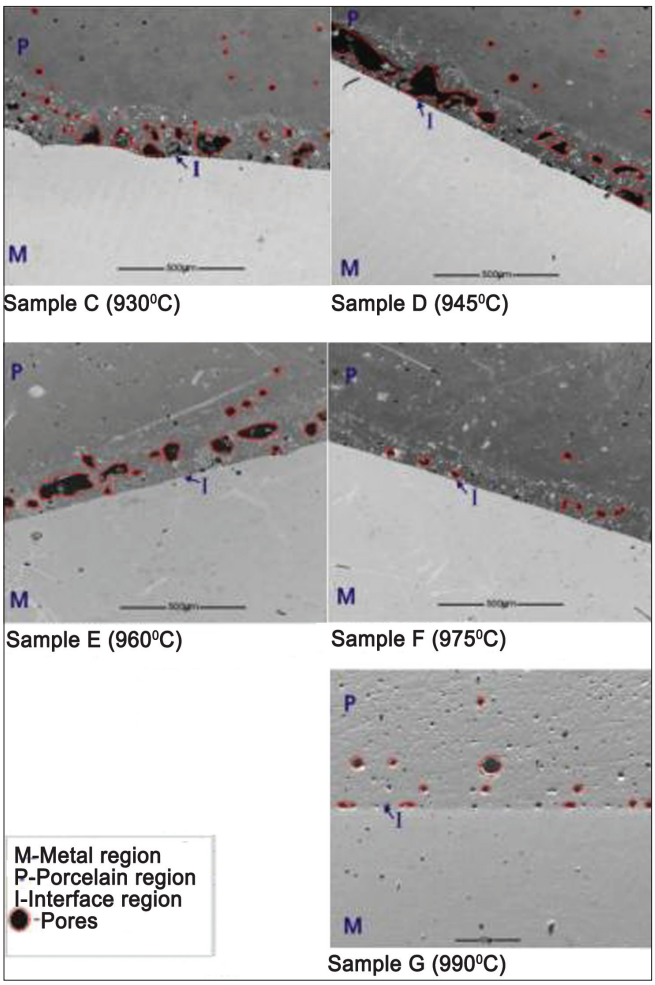

Figure 7: SEM images of porcelain fused to metal samples at different firing temperatures

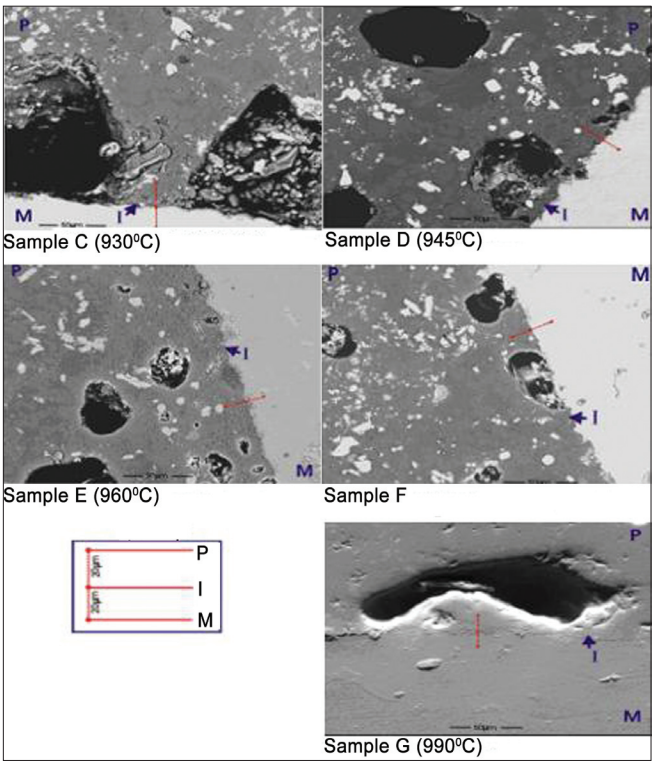

Figure 8: SEM images of porcelain fused to metal samples (opaque porcelain layer) fired at different firing temperatures

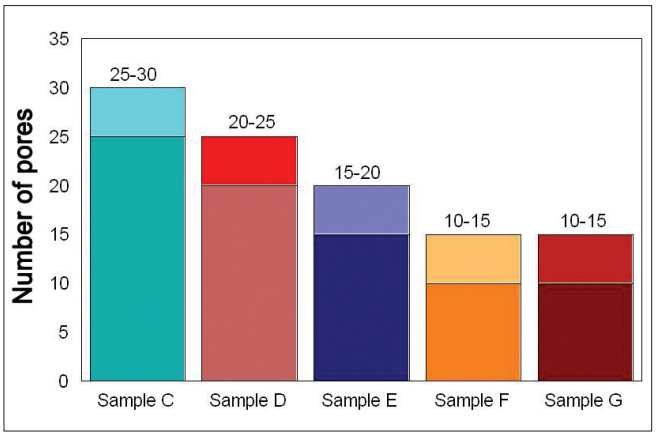

Figure 9: Number of pores of various investigated samples

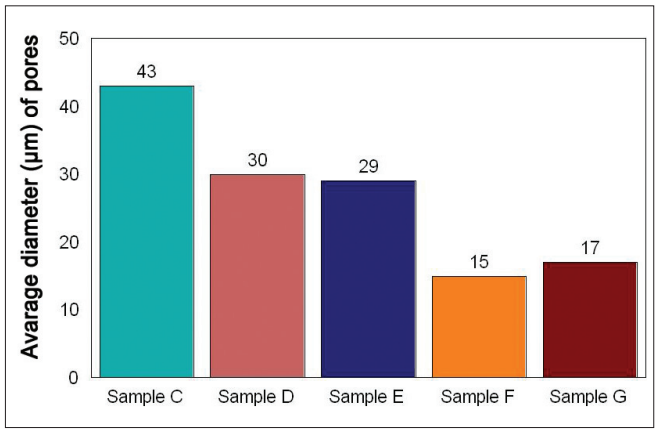

Figure 10: Average diameter of pores investigated in various samples

clearly noted that as the firing temperature was increased, the pores became less in number as well as the size of pores decreased. The least number of pores with least diameter were found at 975°C. It shows that porcelain particles flowed and filled up the air spaces between them optimally at 975°C, which results in better sintering, leading to very few numbers of pores. Another reason of the observation of less number of pores at 975°C might be the optimal match of coefficient of thermal expansion of porcelain and metal.

Also noted was the fact that the pores were present only in the porcelain side and not in the metal side. The pores present in porcelain side are susceptible to crack formation at the edges. These cracks can form when PFM restoration comes under pressure; for example, during mastication, during which an average load of 2 N is transferred along the long axis of PFM crown or bridge. During mastication, the presence of pores can lead to the formation of cracks from its edges. These cracks possibly can coalesce together to form a longer crack. These longer cracks can subsequently propagate parallel to the interface, potentially leading to chipping of the porcelain layer, and hence, failure of the PFM restorations. Slow crack growth phenomenon[25] is most commonly observed in samples with large-sized pores as compared to samples with small-sized pores.

Scope for Future Work

The firing of porcelain on metal in inert atmosphere like argon can be done to observe the influence of different atmosphere on the microstructural changes in the interaction zone. Studies correlating mechanical properties such as strength, with voids number and size can be performed in future to evaluate the nature of porcelain–metal interface.

Conclusions

Based on the experimental investigations of the interaction zone of porcelain fused to metal samples, the following conclusions can be drawn:

1. XRD and SEM – EDS analysis indicated that porcelain–metal interaction occurred during the firing of opaque porcelain layer at varying temperatures of 930°C to 990°C. Another important observation was the presence of pores of varying size, shape, and numbers on the porcelain side at the interaction zone, dependent on firing temperatures of opaque porcelain layers. As the firing temperature was increased, the pores became less in number as well as the size of the pores decreased. The least number of pores with least diameter was found for the sample in which opaque porcelain layer fired at 975°C
2. Several oxides like Cr_2O_3, NiO, and Al_2O_3 and intermetallic compounds ($CrSi_2$, $AlNi_3$) were formed in the interaction zone.
3. The experimental studies indicate that an optimum firing temperature of 975°C is preferred for better adhesion properties of porcelain to Ni–Cr base metal alloy.

References

1. Leone EF, Fairhurst CW. Bond Strength and Mechanical Properties of Dental Porcelain Enamels. J Prosthet Dent 1967;18:155-9.
2. Sced IR, McLean JW. The Strength of Metal/Ceramic Bonds with Base Metals containing Chromium. A preliminary report. Br Dent J 1972;132:232-4.
3. Wagner WC, Asgar K, Bigelow WC, Flinn RA. Effect of Interfacial Variables on Metal-Porcelain Bonding. J Biomed Mater Res 1993;27:531-7.
4. Anusavice KJ, Ringle RD, Fairhurst CW. Bonding Mechanism Evidence in a Ceramic Nonprecious Alloy System. J Biomed Mater Res 1977;11:701-9.
5. Dent RJ, Preston JD, Moffa JP, Caputo A. Effect of Oxidation on Ceramometal Bond Strength. J Prosthet Dent 1982;47:59-62.
6. Knap FJ, Ryge G. Study of Bond Strength of Dental Porcelain Fused to Metal. J Dent Res 1966;45:1047-51.
7. Mackert JR, Ringle RD, Parry EE, Evans AL, Fairhurst CW. The Relationship between Oxide Adherence and Porcelain Metal Bonding. J Dent Res 1988;67:474-8.
8. Rake PC, Goodacre CJ, Moore BK, Munoz CA. Effect of two Opaquing Techniques and two Metal Surface Conditions on Metal-Ceramic Bond Strength. J Prosthet Dent 1995;74:8-17.

9. Tròia MG, Henriques GE, Nòbilo MA, Mesquita MF. The Effect of Thermal Cycling on the Bond Strength of Low-Fusing Porcelain to Commercially Pure Titanium and Titanium-Aluminium-Vanadium Alloy. Dent Mater 2003;19:790-6.
10. Daftary F, Donovan T. Effect of Four Pretreatment Techniques on Porcelain-to-Metal Bond Strength. J Prosthet Dent 1986;56:535-9.
11. Baran GR. Phase Changes in Base Metal Alloys Along Metal-Porcelain Interfaces. J Dent Res 1979;58:2095-104.
12. Williams TR, Winchell PG, Phillips RW. Dental Porcelain/Ni Alloy Interface Reactions and Their Effective Prevention. J Dent Res 1978;57:583-91.
13. Bondioli IR, Bottino MA. Evaluation of Shear Bond Strength at the Interface of Two Porcelains and Pure Titanium Injected into the Casting Mold at three Different Temperatures. J Prosthet Dent 2004;91:541-7.
14. Hofstede TM, Ercoli C, Graser GN, Tallents RH, Moss ME, Zero DT. Influence of Metal Surface Finishing on Porcelain Porosity and Beam Failure Loads at the Metal-Ceramic Interface. J Prosthet Dent 2000;84:309-17.
15. Warpeha WS, Goodkind RJ. Design and Technique Variables Affecting Fracture Resistance of Metal-Ceramic Restorations. J Prosthet Dent 1976;35:291-8.
16. Barghi N, Mckeehan-Whitmer M, Aranda R. Comparison of Fracture Strength of Porcelain-Veneered-to-High Noble and Base Metal Alloys. J Prosthet Dent 1987;57:23-6.
17. Fairhurst CW, Anusavice KJ, Ringle RD, Twiggs SW.Porcelain-Metal Thermal Compatibility. J Dent Res 1981;60:815-9.
18. Bridger DV, Nicholls JI. Distortion of Ceramometal Fixed Partial Dentures during the Firing Cycle. J Prosthet Dent 1981;45:507-14.
19. Stannard JG, Marks L, Kanchanatawewat K. Effect of Multiple Firing on the Bond Strength of Selected Matched Porcelain-Fused-to-Metal Combinations. J Prosthet Dent 1990;63:627-9.
20. Winkler S, Morris HF, Monteiro JM. Changes in Mechanical Properties and Microstructure Following Heat Treatment of a Nickel-Chromium Base Alloy. J Prosthet Dent 1984;52:821-7.
21. Ringle RD, Mackert JR, Fairhurst CW. An X-ray Spectrometric Technique for Measuring Porcelain-Metal Adherence. J Dent Res 1983;62:933-6.
22. Suansuwan N, Swain MV. Adhesion of Porcelain to Titanium and a Titanium Alloy. J Dent 2003;31:509-18.
23. DeHoff PH, Anusavice KJ. Viscoelastic Stress Analysis of Thermally Compatible and Incompatible Metal-Ceramic Systems. Dent Mater 1998;14:237-45.
24. Mackert JR. Dental Ceramics. In: Anusavice KJ, editor. Philips Science Of Dental Materials. 10th ed. Philadelphia: W.B. Saunders Company; 1995. p. 583-616.
25. Craig GR. Ceramics. In: Craig GR, Powers MJ, editors. Restorative Dental Material. 11th ed. New Delhi: Elseviers; 2005. p. 553-71.

Source of Support: Nil, **Conflict of Interest:** None declared.